Journal of Alloys and Compounds 503 (2010) 436–438

Contents lists available at ScienceDirect

Journal of Alloys and Compounds

journal homepage: www.elsevier.com/locate/jallcom

Synthesis and characteristics of Li-doped ZnO powders for p-type ZnO

Bing Wang*, Lidan Tang, Jingang Qi, Huiling Du, Zhenbin Zhang

Department of Materials Physics, Liaoning University of Technology, Shiying Road 169, Jinzhou 121001, China

ARTICLE INFO

Article history:
Received 12 April 2010
Received in revised form 4 May 2010
Accepted 5 May 2010
Available online 11 May 2010

Keywords:
Li-doped ZnO
p-Type
Combustion synthesis method

ABSTRACT

Li-doped zinc oxide (ZnO) powders were synthesized by combustion synthesis method using glycine, urea and metal nitrate as the starting materials. The structural and morphological properties of Li-doped ZnO powders were characterized by TG–DSC, XRD and TEM. Results show that as-prepared powders are crystalline in nature and their average sizes are 0.2–0.4 μm. XPS and XRD results clearly show that Li element had doped into ZnO crystal lattice, which is benefit for fabrication of p-type ZnO films.

1. Introduction

Zinc oxide has attracted much attention as a promising material for short-wavelength optoelectronic devices, such as ultraviolet light emitting diodes and laser diodes, because of its wide band gap (3.37 eV) and large exciton binding energy (60 meV) [1–4]. A key issue in exploring ZnO is the fabrication of p-type ZnO. In recent years, considerable efforts have been made to create p-type ZnO using group-V elements such as N, P, As and Sb [5–8], but their acceptor levels are theoretically identified to be deep with low solubility limits. In contrast to that, group-I species substituting for Zn, such as Li_{Zn}, theoretically possess shallower acceptor levels [9–11]. Furthermore Li element may be the best candidate in producing p-type ZnO due to almost no lattice relaxations around the impurity atom. Nowadays, radio-frequency magnetron sputtering technique has been developed to prepare p-type ZnO films, furthermore metal-doped ZnO films using sputtering method have been fabricated almost from powder target. In this research, Li-doped ZnO powders had been prepared by combustion synthesis method that is a simple, quick, and inexpensive method comparing with other methods [12–14]. The as-prepared ZnO powders are primary materials of p-type ZnO film fabricated by radio frequency magnetron sputtering and lithium atom has been introduced into ZnO crystal that benefit for p-type ZnO film.

2. Experimental procedure

In order to synthesize Li-doped ZnO powders, $Zn(NO_3)_2$ (analytical reagent grade), $LiNO_3$ (analytical reagent grade), glycine (H_2NCH_2COOH, analytical reagent grade), and urea ($CO(NH)_2$, analytical reagent grade) were used as starting materials. Metal nitrates are employed as oxidizing agents. Glycine and urea act as mixed fuels. Table 1 shows the molar ratios of the starting materials that corresponds to the situation of equivalent stoichiometric ratio as equations (1).

$$(1-x)Zn(NO_3)_2 + xLi(NO_3) + 1.337CO(NH_2)_2 + 0.666NH_2{-}CH_2{-}COOH + 1.109O_2 \xrightarrow{\text{combustion}} (1-x)ZnO + (x)0.15Li_2O + 4.339H_2O + 2.665N_2 + 2.669CO_2 \quad (1)$$

These starting materials with required molar ratios were mixed in deionized water to obtain transparent solution. Various Li contents, as listed in Table 1, were studied to investigate the doping effect. These solutions were evaporated quickly and ignited until a self-sustaining and rather fast combustion reaction took off resulting in porous, foamy and fragile materials. Finally these as-prepared materials were then lightly ground for 10 min in corundum bowl to obtain well-crystallized powders.

The structural and morphological of Li-doped ZnO powders were characterized by XRD, TEM and TG–DSC. XRD was carried on to identify phase formation using CuKα radiation at a scanning speed of 2 min^{-1} on a Rigaku Dmax-RB X-ray diffractometer. Observation of morphologies and structures were performed in transmission electron microscopy (TEM) (JEOL-2010, operating at 200 kV), and selected area electron diffraction (SAED). The powders were also studied by simultaneous thermo-gravimetric analysis (TG) and differential scanning calorimetry (DSC) (NETZSC STA409C) with an air-flow and a 20 °C min^{-1} temperature rate. The doping effect was analyzed by X-ray photoelectron spectroscopy (XPS). The XPS analysis was performed using a spectrometer RIBER 200 surface analysis system.

3. Results and discussion

The TG–DSC curve of Li-doped ZnO powder with Li content of 3 at.% (Sample C) is given in Fig. 1. The TG–DSC analysis shows that almost no peaks and no weight loss occur in the curves because the most of the organics are removed during combustion and decomposition reactions of metal nitrates are complete. The TG–DSC results reveal that the as-prepared powders are pure ZnO powders

* Corresponding author. Tel.: +86 0416 4199650.
E-mail address: lgclwb@yahoo.com.cn (B. Wang).

0925-8388/$ – see front matter © 2010 Elsevier B.V. All rights reserved.
doi:10.1016/j.jallcom.2010.05.028

Table 1
The molar ratios of the starting materials.

Sample	$Zn(NO_3)_2$ (mol)	$LiNO_3$ (mol)	H_2NCH_2COOH (mol)	$CO(NH)_2$ (mol)
A	1	0	1.337	0.666
B	0.99	0.01	1.337	0.666
C	0.97	0.03	1.337	0.666
D	0.95	0.05	1.337	0.666

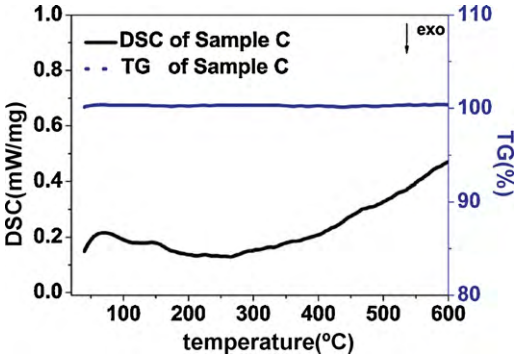

Fig. 1. TG–DSC curve of Li-doped ZnO powder (Sample C).

without other impurities, such as $Zn(NO_3)_2$, $LiNO_3$, H_2NCH_2COOH and $CO(NH)_2$.

Fig. 2 shows the XRD patterns of as-synthesized Li-doped ZnO powders with different Li contents. All the peaks in the figure can be indexed. A search-match database analysis confirms that all of samples reveal a highly crystallized wurtzite structure. This is due to high in situ temperature (>800 °C) [15]. No signals of the metal nitrates are detected by XRD patterns. Also, there is no peak corresponding with the Li_2O. These pure ZnO powders with a highly crystallized wurtzite structure are completely formed in combustion, which agrees with TG–DSC analysis.

The size of the ZnO particles was estimated by applying the Scherrer formula [16] according to the half peak intensity width of the (1 0 0), (0 0 2) and (1 0 1) peaks.

$$d = \frac{0.9\lambda}{B\cos\vartheta}$$

where d is the average particle size in nm, λ is the wavelength of Cu Kα radiation (0.154249 nm), θis the Bragg diffraction angle of the line, and B is the line width at half peak intensity. From this formula,

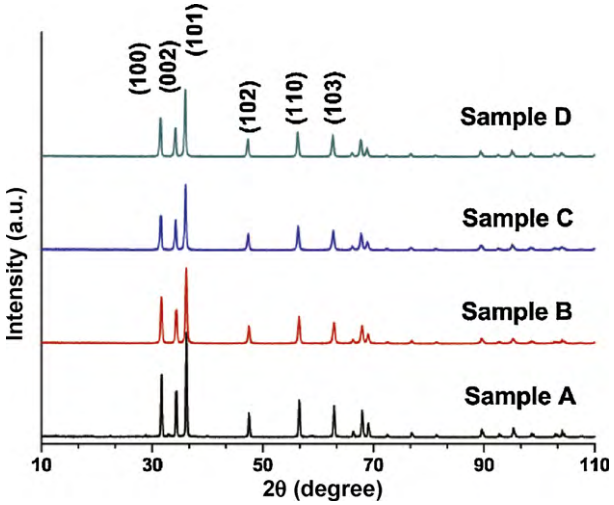

Fig. 2. XRD patterns of Li-doped ZnO powders with different Li contents.

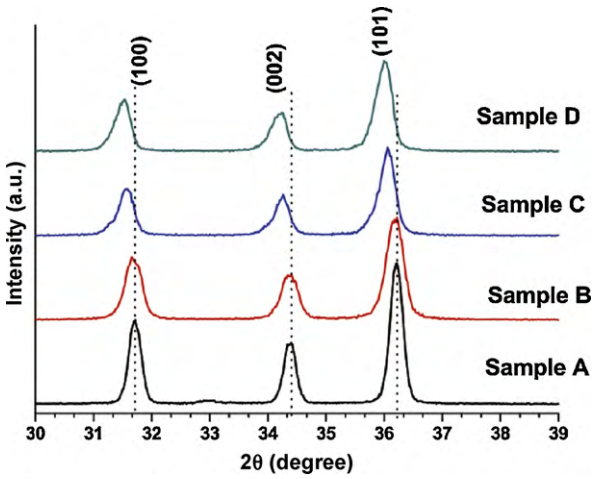

Fig. 3. Low scan run of XRD of Li-doped ZnO powders with different Li contents.

the average sizes of ZnO particles are estimated to be approximately 255 nm, 289 nm, 292 nm and 364 nm, respectively, when Li contents are 0 at.%, 1 at.%, 3 at.% and 5 at.%. The particle sizes are changing with the content of Li element because Li elements had introduced in ZnO crystal to cause lattice dilatation.

To confirm the Li element doped into the ZnO lattice, low scan run of XRD of Li-doped ZnO powders with different Li contents are shown in Fig. 3. These diffraction peaks are (1 0 0), (0 0 2) and (1 0 1), respectively, in the region 2θ 30–39°. These main peaks of Li-doped ZnO are shifted to lower diffraction angel as increasing Li content in ZnO powders. Sample C (ZnO + 3 at.% Li) has the biggest shift of peak position due to more Li element incorporation into ZnO crystal lattice to bring asymmetry of crystal lattice [17,18]. On the other hand the shifting of Sample D is almost equal to that of Sample C because redundant Li element in ZnO is separate from crystal lattice to congregate on the grain boundaries as a second phase that is detrimental to p-type ZnO.

Fig. 4 shows the TEM image and the selected area electron diffraction (SAED) pattern of Li-doped ZnO powder (Sample D). The Li-doped ZnO powder, synthesized at the same condition, consists of small ellipse-like particles with an average size of approximately 380 nm that is close to the calculation results using the Scherrer formula. The selected area electron diffraction (SAED)

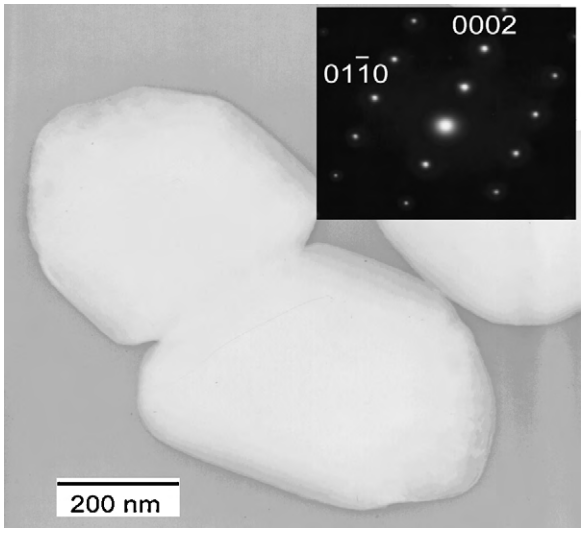

Fig. 4. TEM image and the selected area electron diffraction pattern of Li-doped ZnO powder (Sample D).

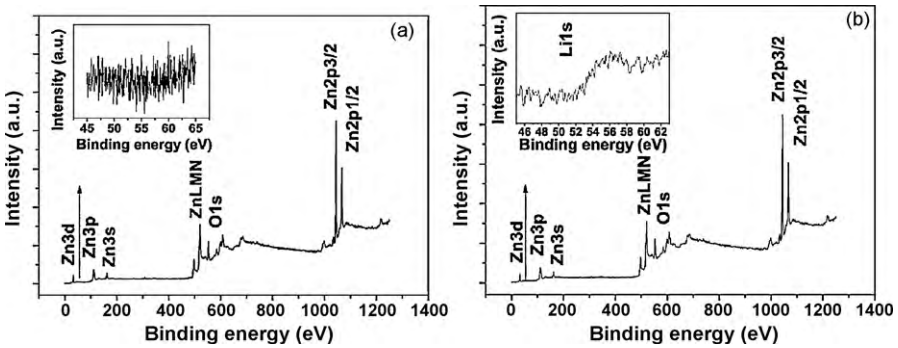

Fig. 5. XPS pattern of Li-doped ZnO powders with different Li contents. (a) Sample C and (b) Sample D.

pattern of Li-doped ZnO powder is shown in the inset of Fig. 4. The spot diffraction pattern further confirmed the XRD results that the Li-doped ZnO particles have highly crystallized wurzite structure.

In order to gain a deeper insight into the Li element doped into the ZnO lattice, the chemical state was measured by XPS. Fig. 5(a) presents the indicated XPS pattern of Li-doped ZnO powders with Li content of 3 at.% (Sample C). The Zn2p3/2 and Zn2p1/2 binding energies of Li-doped ZnO powder are 1021.9 eV and 1044.9 eV, respectively. The Zn2p3/2 and Zn2p1/2 binding energies of both samples shifting to lower energy show that many impurities may occur in ZnO crystal [19]. The peak at 530 eV corresponds to the binding energy of O1s. However the lithium peak is not seen in XPS survey spectrums and high resolution Li1s XPS spectrum (see inset). It may be due to Li element incorporation into ZnO crystal lattice when the Li content is lower than 3 at.%, which agrees with the XRD results. The process of doping could be explained as following [20]:

$$Li_2O \rightarrow (1-x)Li'_{Zn} + (1+x)Li_i^+ + O_O$$

where Li_i^+ and Li'_{Zn} are Li element occupying an interstitial site and a substitutional site in ZnO powders, respectively. O_O is O element occupying crystal lattice site. A consequence of the Zn^{2+} ion being replaced by Li^+ introduces an acceptor level into the crystal. With Li content increasing (5 at.%) lithium peaks (Li1s) are observed in high resolution Li1s XPS spectrum (seen in Fig. 5(b)). The results suggested that redundant Li elements separated from crystal lattice to congregate on the grain boundaries as the second phases in ZnO powders that is detrimental to the carrier mobility in p-type ZnO. As a result, Sample C is the best sputtering raw material of p-type ZnO film because more Li element is introduced into ZnO crystal and not the second phases.

4. Conclusion

These Li-doped ZnO powders had been prepared by combustion synthesis. These as-prepared powders showed a highly crystallized wurtzite structure and small ellipse-like particles with an average size of 0.2–0.4 μm. The Li-doped ZnO powder with Li doped content of 3 at.% is the best raw material of p-type ZnO film due to more Li element incorporated into ZnO crystal lattice.

References

[1] U. Ozgur, Y.I. Alivov, C. Liu, A. Teke, M.A. Reshchikov, S. Dogan, V. Avrutin, S.-J. Cho, H. Morkoc, J. Appl. Phys. 98 (2005) 041301.
[2] T. Aoki, Y. Hatanaka, D.C. Look, Appl. Phys. Lett. 76 (2000) 3257.
[3] J.J. Qi, Y. Zhang, Y.H. Huang, Q.L. Liao, J. Liu, Appl. Phys. Lett. 89 (2006) 252115.
[4] Z.K. Tang, G.K.L. Wong, P. Yu, M. Kawasaki, A. Ohtomo, H. Koinuma, Y. Segawa, Appl. Phys. Lett. 72 (1998) 3270.
[5] M. Joseph, H. Tabata, H. Saeki, K. Ueda, T. Kawai, Physica B 302–303 (2001) 140–148.
[6] F.X. Xiu, Z. Yang, L.J. Mandalapu, J.L. Liu, Appl. Phys. Lett. 88 (2006) 052106.
[7] D.C. Look, G.M. Renlund, R.H. Burgener, J.R. Sizelove, Appl. Phys. Lett. 85 (2004) 5269–5271, 22.
[8] L.J. Mandalapu, F.X. Xiu, Z. Yang, D.T. Zhao, J.L. Liu, Appl. Phys. Lett. 88 (2006) 112108.
[9] Y.J. Zeng, Z.Z. Ye, W.Z. Xu, D.Y. Li, J.G. Lu, L.P. Zhu, B.H. Zhao, Appl. Phys. Lett. 88 (2006) 062107.
[10] L.L. Chen, H.P. He, Z.Z. Ye, Chem. Phys. Lett. 420 (2006) 358–361.
[11] A. Galal, B.A. Mohamed, M. bd El-Moiz, Rashad, Physica B 370 (2005) 58.
[12] B.W. Liu, Y. Zhang, J. Alloys Compd. 453 (2008) 418.
[13] C.S. Lin, C.C. Hwang, W.H. Lee, et al., Mater. Sci. Eng. B 140 (1–2) (2007) 31.
[14] S. Ekambaram, Y. Iikubo, A. Kudo, J. Alloy Compd. 433 (2007) 237–240.
[15] C.C. Hwang, T.Y. Wu, Mater. Sci. Eng. B 111 (2–3) (2004) 197.
[16] J.F. Lu, Q.W. Zhang, J. Wang, F. Saito, M. Uchida, Powder Technol. 162 (2006) 33–37.
[17] S.H. Jeong, B.N. Park, S.B. Lee, J.H. Boo, Thin Solid Films 516 (16) (2008) 5586–5589.
[18] A. Galal, A.B. Mohamed, M. Abd El-Moiz, Rashad, Phys. B: Condens. Matter 370 (1–4) (2005) 158–167.
[19] B.E. Jun, Y.S. Kim, H.J. Park, S.B. Kim, H.K. Yang, J.H. Park, B.C. Choi, J.H. Jeong, Thin Solid Films 516 (16) (2007) 5266–5271.
[20] A. Yavuz Oral, Z. Banu Bahs, M. Hasan Aslan, Appl. Surf. Sci. 253 (2007) 4593.